Anomalous grain growth in the surface region of a nanocrystalline CeO_2 film under low-temperature heavy ion irradiation

P. D. Edmondson,[1,2,*] Y. Zhang,[2,3] S. Moll,[4] T. Varga,[5] F. Namavar,[6] and W. J. Weber[2,3]

[1]*Department of Materials, University of Oxford, Parks Road, Oxford, OX1 3PH, United Kingdom*

[2]*Materials Science and Technology Division, Oak Ridge National Laboratory, Oak Ridge, Tennessee 37831, USA*

[3]*Department of Materials Science and Engineering, University of Tennessee, Knoxville, Tennessee 37996, USA*

[4]*CEA-DEN, Service de Recherches de Métallurgie Physique, Centre d'Études de Saclay, 91191 Gif-sur-Yvette Cedex, France*

[5]*Environmental Molecular Sciences Laboratory, Pacific Northwest National Laboratory, P.O. Box 999, Richland, Washington 99352, USA*

[6]*University of Nebraska Medical Center, Omaha, Nebraska 68198, USA*

(Received 3 February 2012; revised manuscript received 17 April 2012; published 15 June 2012)

Grain growth and phase stability of nanocrystalline ceria are investigated under ion irradiation at different temperatures. Irradiations at temperatures of 300 and 400 K result in uniform grain growth throughout the film. Anomalous grain growth is observed in thin films of nanocrystalline ceria under 3-MeV Au^+ irradiation at 160 K. At this low temperature, significant grain growth is observed within 100 nm from the surface, and no obvious growth is detected in the rest of the films. While the grain growth is attributed to a defect-stimulated mechanism at room temperature and above, a defect diffusion-limited mechanism is significant at low temperatures with the primary defect responsible being the oxygen vacancy. The nanocrystalline grains remain in the cubic phase regardless of defect kinetics.

DOI: 10.1103/PhysRevB.85.214113 PACS number(s): 61.80.−x, 61.82.Rx, 61.72.−y

I. INTRODUCTION

Thin films of binary oxide ceramics, such as zirconia (ZrO_2) and ceria (CeO_2) are technologically important materials. Due to their exceptional ionic conductivity, they are particularly attractive for use in solid oxide fuel cells.[1,2] However, it has been suggested that nanocrystalline films may be used due to the enhancement of the material properties and the ability to tailor those properties with grain size.[3,4] A 4-orders-of-magnitude increase in the electrical conductivity of CeO_2 has been observed when the grain size is reduced from the micro- to the nanocrystalline scale.[5] Recently, the possibility to achieve higher ionic conductivity in nanocrystalline zirconia has been discussed.[6] It is well known that the ionic conductivity of zirconia is via an oxygen vacancy mechanism, and as such, enhanced conductivity may be achieved by controlling the oxygen vacancy concentration. In a later paper, it was demonstrated that oxygen concentration or a saturation of oxygen vacancies may be controlled in zirconia film by ion beams while maintaining nanosized grains.[7] This demonstrated the novel use of ion beams to effectively defect engineer materials to enhance their properties.

In this paper, thin films of nanocrystalline ceria have been irradiated with 3-MeV Au^+ ions at 160, 300, and 400 K in order to evaluate the response of the material to energy deposition and to examine if ion-beam manipulation of the thin films may be used to enhance the properties of the films.

II. EXPERIMENTAL METHODS

Thin films, approximately 330-nm thick nanocrystalline CeO_2, have been deposited onto a (001) silicon substrate using an ion-beam-assisted-deposition (IBAD) technique chronicled elsewhere.[8] The average initial grain diameter is ∼6 nm. These films have previously been shown to be in the cubic form.[9]

The films were then irradiated with 3-MeV Au^+ ions at temperatures ranging between 160 and 400 K and up to doses of ∼35 displacements per atom (dpa) using the 3-MV tandem accelerator facilities located at the Environmental Molecular Sciences Laboratory (EMSL) at Pacific Northwest National Laboratory. Particular care was taken during the 160-K experiment so as to ensure that thermal steady state was achieved prior to ion bombardment. The ion energy was chosen such that the energy deposition into the CeO_2 film was maximized while minimizing the number of ions implanted into the film. Following irradiation, the thin films were examined using a combination of glancing incidence x-ray diffraction (GIXRD), Rutherford backscattering spectroscopy (RBS), and cross-sectional transmission electron microscopy (XTEM). The GIXRD was performed to determine nominal grain size using a Philips X'Pert diffractometer with Cu $K_{\alpha 1}$ x rays. The average grain size of the films was determined using pseudo-Voigt profiles of the main diffraction peaks. The results from the RBS measurements of the as-deposited and irradiated samples are used to determine the film stoichiometry and thickness (in atom cm^{-2}). Specimens to be examined in XTEM were prepared using a tripod polishing technique in which the samples are mechanically thinned to a thickness of 15–20 μm before ion milling to perforation using a Gatan precision ion polishing system with beam energy reduced from 4.5 to 3 keV. A JEOL 2010 transmission electron microscope (TEM) operating at 200 keV was used to image the specimens.

III. RESULTS

A. As-deposited film

TEM micrographs of the as-deposited material are shown in Fig. 1. The diffraction contrast image in Fig. 1(a) shows the nanostructured ceria (NSC) film on the top of a silicon substrate with an approximately 5-nm buffer layer of SiO_2. The structure of the NSC film appears to be uniform throughout with no abrupt changes in contrast. The selected area electron diffraction (SAED) pattern shown in Fig. 1(b) indicates that

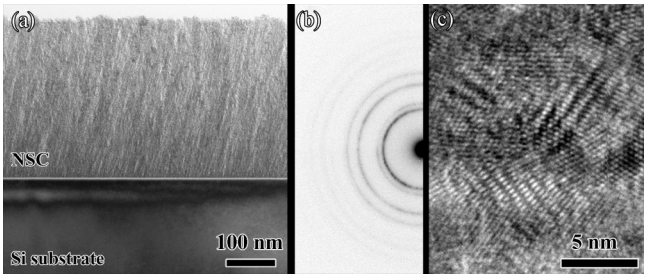

FIG. 1. (a) XTEM, (b) SAED, and (c) HREM of the as-deposited nanostructured ceria film.

the film is polycrystalline in nature and that it is in the cubic phase. High-resolution XTEM (HREM) reveals that the film is composed of highly crystalline nanometer-sized grains with GIXRD indicating an average grain size of ∼6 nm. No amorphous material is observed in either the TEM or the GIXRD results.

B. Irradiation of the films at 160 K

A series of XTEM micrographs of the film irradiated with 3-MeV Au^+ ions at a temperature of 160 K up to a total dose of 10.8 dpa is given in Fig. 2. The series in Figs. 2(a)–2(c) shows diffraction contrast, SAED, and HREM (from a near-surface region) images taken from the sample irradiated with a dose of 0.54 dpa. It is clear that some ion-beam modification of the film has occurred. This is manifested as an apparent

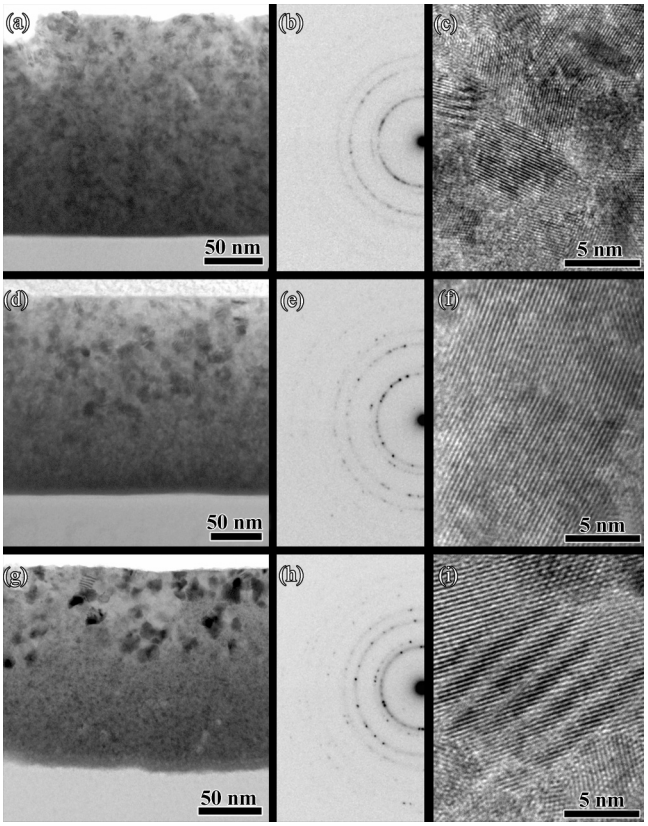

FIG. 2. TEM, SAED, and HREM images of the NSC film irradiated at 160 K at doses of (a)–(c) 0.54, (d)–(f) 3.62, and (g)–(i) 10.8 dpa, respectively.

grain refinement evidenced by the change in appearance of the NSC film itself, the sharpening of the SAED pattern with individual diffraction spots beginning to emerge, and individual nanocrystalline grains becoming more discernible in the HREM image. GIXRD showed that the average grain size of this film was ∼5.7 nm.

The series of images taken from a film irradiated with a dose of 3.62 dpa is shown in Figs. 2(d)–2(f). In comparison with the 0.54-dpa result, grain refinement continues as shown in the SAED pattern. The XTEM image shows that the near-surface region of the film has undergone some ion-beam-induced modification with the grains in this region having undergone significant growth. The HREM image shown in Fig. 2(f) is taken from a grain near this surface region. This HREM image shows that the grains are still highly crystalline. The average grain size determined by GIXRD was found to be ∼9 nm.

Images recorded from the film irradiated at 10.8 dpa are shown in Figs. 2(g)–2(i) in which it is evident again that the nanocrystalline grains in the surface region of the film have undergone a significant modification. The average grain size of the film was determined by XTEM to be ∼9.2 nm, but it is clearly evident that this is not homogeneous throughout the film with significantly larger grains being formed at the surface. It is worth noting here that the grains toward the NSC/Si interface region did not appear to alter much in their structure, retaining the same approximate size and phase.

Increasing the dose to ∼35 dpa resulted in no further major modifications to the film observed in XTEM, but the GIXRD revealed that a continued minor growth of the grains occurred as shown in Fig. 3.

C. Irradiation of the films at elevated temperatures

XTEM images taken from the film irradiated at a temperature of 300 K are shown in Fig. 4. The series in Figs. 4(a)–4(c) are taken from the film irradiated with 0.54 dpa, whereas, the series in Figs. 4(d)–4(f) are from the film exposed with a dose of ∼35 dpa. Uniform grain growth throughout the film is in stark contrast to that of the film irradiated at a temperature of 160 K. Similar evolution of the film microstructure is observed for irradiations performed at 400 K. The average grain size increases at a significantly enhanced rate in comparison with the 160-K irradiation as shown in Fig. 3. It is worth noting

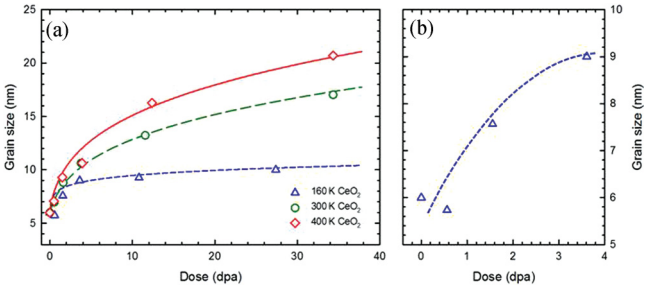

FIG. 3. (Color online) (a) Graph showing irradiation-induced grain growth as a function of dose, as calculated by GIXRD, for the samples irradiated at 160, 300, and 400 K. (b) Magnified region of the low-dose 160-K irradiation-induced grain growth demonstrating the rapid growth with low doses, followed by less rapid growth. The lines serve to guide the eye.

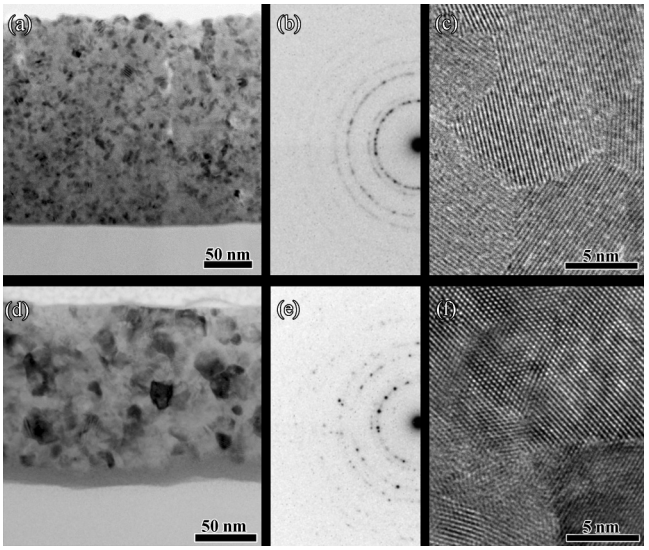

FIG. 4. TEM, SAED, and HREM images of the NSC film irradiated at 300 K at doses of (a)–(c) 0.54 and (d)–(f) 35 dpa, respectively.

that the grain growth is isotropic here, whereas, in the case of irradiated thin films of nanocrystalline zirconia, the grain growth is highly anisotropic.[10,11]

In both the 160- and 300-K irradiations shown in Figs. 2 and 4, there is an apparent reduction in the thickness of the film. The difference in the thickness of the films is attributed to the nonuniform film deposition and irradiation-induced densification. In order to evaluate possible sputtering of the target material, an experiment was performed. A holder was designed in which TEM carbon-foil grids were placed at a constant radius from the sample at angles of 15°, 30°, 45°, and 60° relative to the incoming ion beam, similar to the work of Birtcher *et al.*[12] Following irradiation with a total dose of 108 dpa, the foils were removed and were examined in the TEM. No evidence of sputtering was observed. The experimental determined film density of the as-deposited films from the RBS and TEM results is 6.3 g cm^{-3},[9] which is much less then the theoretical density of 7.215 g cm^{-3}. The low film density is attributed to the porosity induced by the IBAD technique. Comparing the as-deposited and irradiated samples, the GIXRD, RBS, and TEM results suggest that, within experimental uncertainties, there are no phase changes, no loss of Ce content, but a significant reduction in film thickness. The irradiation-induced densification is mainly attributed to an ion-hammering effect under high-dose irradiation, similar to electron hammering,[13] that reduces the film porosity. The density of cubic CeO_2 in the grains is expected to be close to the theoretical density, whereas, the change in the porosity has a significant impact on defect migration and grain growth under ion irradiation.

IV. DISCUSSION

From the results shown above, the difference between the elevated- (300- and 400-K) and cryogenic-temperature (160-K) irradiations are clear—grain growth occurs only in the top half of the film under the 160-K irradiation but throughout the whole film in the elevated-temperature irradiations. Although it has previously been shown that the grain growth under the 300- and 400-K irradiation occurs due to a defect-stimulated mechanism,[11] the dominant defect responsible for this anomalous growth at 160 K has not yet been identified. The temperature-dependent grain growth clearly shows that there is a thermal component to the grain growth as seen in the change in grain growth rate in Fig. 3 where the grain growth is enhanced at 400 K compared to that at 300 K. The growth rate at 160 K is apparently severely constrained. An as-deposited ceria film was annealed at 400 K for 5 h, and no grain growth was observed suggesting that thermal growth at 400 K is negligible. A band of contrast is observed at the interface between the film and the substrate in Figs. 2(g) and 4(d). This band of contrast results from the ion-beam-induced chemical mixing of the film and the substrate. No evidence was found of Si existing in the film outside of the band of contrast region using RBS, secondary ion mass spectroscopy, and scanning TEM-energy dispersive spectroscopy techniques, therefore, the argument of Si coupled to defects traveling upstream that may affect the grain growth can be ruled out. Additionally, it may be that strain or stress fields induced by the irradiation could further facilitate the grain growth. However, the GIXRD results indicate that stress/strain is alleviated at low-dose (∼0.5-dpa) levels and, at which point, is either completely removed or is in a constant steady-state condition, and as such, stress/strain would not be expected to be a dominant factor in the grain growth observed.

The faster grain growth at higher temperatures suggests that ion-beam-induced grain growth in CeO_2 is a temperature-dependent irradiation-enhanced process. The XTEM images of the sample irradiated at 160 K (Fig. 2) shows that the near-surface region undergoes significant grain growth, whereas, the near-interface region does not. This indicates that the process of grain growth in this system is a thermodynamically controlled defect-stimulated process.

During the ion-irradiation process, a nonequilibrium number of defects is produced in the system. These defects may be cation Frenkel pairs, anion Frenkel pairs, or Schottky defects. As the defect production is dominated by ballistic processes [with a negligible thermal rate component due to the relatively high formation energies of defects in CeO_2 (Ref. 14)], the dose rate at which defects are introduced into the system is not the primary driving mechanism behind the grain growth. Given that the grain growth rate is observed to be highly temperature dependent, it is necessary to look toward the diffusion of different defects within the film.

Computational studies of the activation energy for migration and the diffusion coefficients have shown that the cerium interstitials and vacancies are extremely stable, whereas, the oxygen interstitials are metastable and the oxygen vacancies are highly mobile.[14] A summary of the activation energies and diffusion coefficients is given in Table I.

Irradiation at elevated temperatures (300 and 400 K) results in the formation of defects along the ion tracks that, with the low activation energy for oxygen vacancy migration of 0.52 eV,[14] may readily diffuse throughout the material. This may also be enhanced somewhat along the grain boundaries.[10] More rapid grain growth observed at low-dose levels may be attributed to both mobile oxygen vacancies and interstitials

TABLE I. Cerium and oxygen diffusion coefficients and activation energies for migration for interstitials and vacancies as calculated using molecular dynamics (from Ref. 14).

	Cerium		Oxygen	
	Interstitial	Vacancy	Interstitial	Vacancy
D_0 (10^{-5} cm^2 s^{-1})			331 ± 12	5.4 ± 0.4
$E_{\text{Migration}}$ (eV)	6.1	5.3	1.13 ± 0.05	0.52 ± 0.01

within grains and at interfaces. Whereas, both the free surface and the interface may act as sinks for the migrating defects, a previous paper has shown that the free surface may act as a preferential sink that may enhance any microstructural changes.[15] Therefore, in the mechanism presented here, oxygen vacancies produced during the ion irradiation may readily diffuse through the film. Upon reaching the free surface of the film, they are annihilated. This results in the film entering into a metastable defected energy state. As the concentration of defects that are annihilated at the free surface reaches a critical value, the free energy of the film is increased to such an extent that the nanocrystalline grains of the film must follow an energy pathway by which the energy of the system is reduced. The energy reduction in the film occurs in the form of growth of the nanocrystalline grains where grain boundaries may inject oxygen vacancies into the grain for charge balance, similar to the process demonstrated in a metallic system.[16] This grain growth occurs at the expense of neighboring grains that have grain boundaries in the higher-energy asymmetric state, rather than those that are in the more energetically favorable symmetric state. In terms of the thermodynamics of the system, the entropy of the system is increased during the irradiation. The reduction in the free energy of the system occurs through the occurrence of two processes: First, the grain growth occurs in which the relative volume of the grain boundaries is reduced in the system aiding to reduce the entropy via a reduction in the misorientation volume of the system; and second, by switching the grain-boundary structure from the higher-energy asymmetric state to the lower-energy symmetric state. This transition is facilitated by the diffusion of the oxygen vacancies to the free surface.

During the irradiation at 160 K, the grain growth is somewhat muted in comparison with the higher-temperature cases. Due to limited migration length at low temperatures, there are fewer oxygen vacancies diffusing to, and being annihilated at, the surface. Additionally, since there is no significant change in the lattice parameter, O interstitials and vacancies must maintain stoichiometry and charge balance. As such, the loss of oxygen vacancies at the surface must only be temporary and that injection of oxygen vacancies must occur in order to maintain charge and structural balance. However, this is expected to be delayed somewhat due to the low temperature of the film during irradiation, and it is this temporary imbalance in charge and structure that allows for the grains to undergo growth. Only those defects in relatively close proximity to the surface may diffuse to the surface, such as those due to the local thermal effects from ion-solid interaction resulting from both the electronic and the nuclear energy deposition. This increase in temperature would allow the oxygen vacancies to diffuse along the collision paths toward the surface.[17] The different dose dependencies of grain growth at different temperatures shown in Fig. 3 further support the additional defect diffusion-limited growth mechanism. Two growth trends can be observed at doses below a few dpa or above. At irradiation doses up to ~4 dpa, similar grain growth behavior is observed under the 160-, 300-, and 400-K irradiation with fast growth at higher temperatures, whereas, constrained growth under high-dose irradiation is evident at 160 K as compared with the 300- and 400-K results. As discussed above, there is significant reduction in film thickness resulting from the reduced porosity that is attributed to irradiation-induced densification. At low doses, due to the porosity, there will exist a relatively large surface area (the sample surface and surface of some of the nanosized grains), and grain growth will less likely be limited by the diffusion-limited growth mechanism. With an increase in the irradiation above a few dpa, porosity is reduced as shown by the reduction in the film thickness and improved sharpness of the grain boundaries in the irradiated samples in Figs. 1, 2, and 4, and the role of defect diffusion-limited growth mechanism becomes dominant.

It is also observed that the interface between the grains that undergo growth and those toward the interface is not planar and has a wavelike appearance as seen in Fig. 2. This can be attributed to the fairly strong directional dependence on the diffusion of the oxygen vacancies in ceria.[14] Molecular-dynamics simulations have demonstrated that oxygen vacancies undergo a thermal diffusion process preferentially along the [100] direction.[14] Given the random nature of the nanocrystalline film, it is to be expected that there is a random distribution of grains with specific orientations in the film. The grains within the diffusion path length that are orientated in the [100] direction will undergo grain growth; those in higher-order orientations will have a suppressed grain growth. However, it may also be expected that diffusing vacancies may also migrate across or along grain boundaries to reach the surface. This may also enhance the effect of the surface on grain growth.

It may also be reasonable to assume that the microstructure of the nanocrystalline grains near the surface of the film under the 160-K irradiation may undergo a microstructural change. GIXRD patterns have shown the phase during the 300- and 400-K irradiations to remain cubic.[9] However, as with the anomalous grain growth observed, since the GIXRD result presents an average result of all the grains throughout the film, measurements of the lattice spacing of the grains visible in HREM have been performed in order to identify the phase. A typical line-scan profile from grains in the as-deposited near-surface 160-K 10.8-dpa and near-interface 160-K 10.8-dpa samples are shown in Fig. 5. The insets are the average fringe spacing. The as-deposited sample is shown to be, by GIXRD, in the cubic phase, and the measured lattice spacing is equivalent to the d_{111} spacing. Both the near-surface and the near-interface results are the same (within the error), and as such, it can be said that the nanocrystalline grains are cubic in phase and undergo no unit-cell deformation. It is also interesting to note that there is essentially no change in the lattice parameter indicating that the film is relatively stress free and that there are no density changes in the ceria grains. This is somewhat surprising given that, during similar experiments

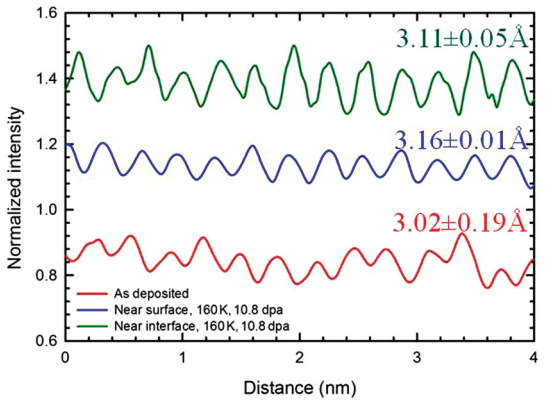

FIG. 5. (Color online) Normalized lattice fringe intensity profiles for the as-deposited, near-surface 160-K 10.8-dpa and near interface 160-K 10.8-dpa samples. The insets are the average d_{111} spacing as measured by the intensity profiles of, at least, five grains.

on nanocrystalline zirconia, a shift in the lattice parameter was observed, relating to the formation of oxygen vacancies in that film.[7]

V. CONCLUSION

Thin films of nanocrystalline ceria have been irradiated with 3-MeV Au^+ ions at temperatures in the range of 160 to 400 K to study the effect of irradiation on the microstructure of the film. A uniform grain growth was observed to occur throughout the film during irradiation at 300 and 400 K, whereas, only the top half of the film underwent grain growth during irradiation at 160 K. It is proposed that the grain growth results from a defect-stimulated diffusion-limited growth mechanism in which the diffusion of defects to the free surface of the film is the driving force. The diffusion of defects to the free surface of the film results in a metastable energy state of the film. When the energy state reaches above a critical value, the grains undergo a growth in order to reduce the overall system energy at the expense of the asymmetric grain boundaries. It is suggested that the dominant defect responsible for this growth is the oxygen vacancy and that this defect preferentially diffuses along the [100] direction. The temperature-dependent diffusion of the oxygen vacancy is significantly suppressed at 160 K, which leads to the anomalous grain growth in the near-surface region.

ACKNOWLEDGMENTS

This work was supported as part of the Materials Science of Actinides, an Energy Frontier Research Center funded by the US Department of Energy, Office of Science, Office of Basic Energy Sciences, Materials Sciences and Engineering Division. A portion of the research was performed at the EMSL, a national scientific user facility sponsored by the Department of Energy's Office of Biological and Environmental Research and located at Pacific Northwest National Laboratory.

*Corresponding author: philip.edmondson@materials.ox.ac.uk

[1]B. W. Busch, W. H. Schulte, E. Garfunkel, T. Gustafsson, W. Qi, R. Nieh, and J. Lee, Phys. Rev. B **62**, R13290 (2000).
[2]G. Knöner, K. Reimann, R. Röwer, U. Södervall, and H.-E. Schaefer, Proc. Natl. Acad. Sci. USA **100**, 3870 (2003).
[3]A. P. Alivisatos, Science **271**, 933 (1996).
[4]M. V. Kovalenko, M. Scheele, and D. V. Talapin, Science **324**, 1417 (2009).
[5]Y. M. Chiang, E. B. Lavik, I. Kosacki, H. L. Tuller, and J. Y. Ying, Appl. Phys. Lett. **69**, 185 (1996).
[6]X. Guo, Scr. Mater. **65**, 96 (2011).
[7]P. D. Edmondson, W. J. Weber, F. Namavar, and Y. Zhang, Scr. Mater. **65**, 675 (2011).
[8]F. Namavar, C. L. Cheung, R. F. Sabirianov, W.-N. Mei, X. C. Zeng, G. Wang, H. Haider, and K. L. Garvin, Nano Lett. **8**, 988 (2008).
[9]Y. Zhang, P. D. Edmondson, T. Varga, S. Moll, F. Namavar, C. Lan, and W. J. Weber, Phys. Chem. Chem. Phys. **13**, 11946 (2011).
[10]P. D. Edmondson, Y. Zhang, F. Namavar, C. M. Wang, Z. Zhu, and W. J. Weber, Nucl. Instrum. Methods Phys. Res. B **269**, 126 (2011).
[11]Y. Zhang, W. Jiang, C. Wang, F. Namavar, P. D. Edmondson, Z. Zhu, F. Gao, J. Lian, and W. J. Weber, Phys. Rev. B **82**, 184105 (2010).
[12]R. C. Birtcher, A. W. McCormick, P. M. Baldo, N. Toyoda, I. Yamada, and J. Matsuo, Nucl. Instrum. Methods Phys. Res. B **206**, 851 (2003).
[13]I. T. Bae, Y. Zhang, W. J. Weber, M. Ishimaru, Y. Hirotsu, and M. Higuchi, Nucl. Instrum. Methods Phys. Res. B **266**, 3037 (2008).
[14]A. Guglielmetti, A. Chartier, L. v. Brutzel, J.-P. Crocombette, K. Yasuda, C. Meis, and S. Matsumura, Nucl. Instrum. Methods Phys. Res. B **266**, 5120 (2008).
[15]J. S. Williams, X. Zhu, M. C. Ridgway, M. J. Conway, B. C. Williams, F. Fortuna, M.-O. Ruault, and H. Bernas, Appl. Phys. Lett. **77**, 4280 (2000).
[16]X.-M. Bai, A. F. Voter, R. G. Hoagland, M. Nastasi, and B. P. Uberuaga, Science **327**, 1631 (2010).
[17]S. Moll, L. Thomé, L. Vincent, F. Garrido, G. Sattonnay, T. Thomé, J. Jagielski, and J. M. Costantini, J. Appl. Phys. **105**, 023512 (2009).